

文章编号 : 1003-501X(2008)02-0061-05

Remote Sensing Image Compression Algorithm Based on Wavelet Sub-bands Entropy

SUI Yu-ping^{1,2}, YANG Cheng-yu^{1,2}, LIU Yan-jun^{1,2}, WANG Jun¹, WEI Zhong-hui¹, HE Xin¹

(1. Changchun Institute of Optics, Fine Mechanics and Physics, Chinese Academy of Sciences, Changchun 130033, China;

2. Graduate School of Chinese Academy of Sciences, Beijing 100039, China)

Abstract: A high-performance lossy compression algorithm was proposed for remote sensing image compression based on bit allocation using sub-bands entropy. After decomposing the remote sensing image by using wavelet lifting scheme, the distribution of energy percentage and entropy of high frequency sub-bands were analyzed. A novel bit allocation method using the entropy was proposed. Uniform scalar quantification was implemented for each high frequency sub-band. Bit plane encoding followed and included two parts. The coordinates of non-zero coefficients were registered in the most significant bit plane, and run-length encoding and Huffman encoding were adopted for other bit planes. Experimental results show that the compression scheme performs well on a set of test remote sensing images including complicated texture images and relative planar ones. The Peak Signal to Noise Ratio (PSNR) is all higher than 34dB. However, the Compression Ratio (CR) depends on image's complicated degree.

Key words: remote sensing image; wavelet compression; bit allocation; entropy

CLC number: TP751

Document code: A

一种基于小波子带熵的遥感图像压缩算法

隋玉萍^{1,2}, 杨成禹^{1,2}, 刘岩俊^{1,2}, 王 军¹, 魏仲慧¹, 何 昕¹

(1. 中国科学院长春光学精密机械与物理研究所, 长春 130033 ;

2. 中国科学院研究生院, 北京 100039)

摘要: 提出了一种使用小波子带熵进行比特分配的遥感图像压缩算法。对遥感图像进行小波提升分解后, 分析了各高频子带能量百分比及其熵的变化趋势, 在此基础上提出了一种新的快速比特分配方法 - 使用子带熵进行比特分配。然后对各个高频子带进行均匀量化, 量化后的数据采用比特平面编码。对最高比特平面只记录该比特平面中非零系数的坐标, 其它比特平面采用行程编码和 Huffman 编码方法进行压缩。实验结果表明, 纹理复杂以及相对平坦的遥感图像使用该算法压缩后都可以获得很好的重构图像质量, 峰值信噪比均大于 34dB, 而压缩比则与图像的复杂程度有关。

关键词: 遥感图像; 小波压缩; 比特分配; 熵

1 Introduction

Remote sensing images acquired on board spacecrafts such as earth observation satellites and scientific probes, provide huge volume of data. Further more, the data volume increases by geometric series with the development of imaging equipments. Usually these data are stored on board during invisible period and transmitted to the ground later. But because of the stringent limitations of equipments' mass and power on board

收稿日期: 2007-03-20; 收到修改稿日期: 2007-11-20

基金项目: 国家 863 计划项目

作者简介: 隋玉萍(1980-), 女(汉族), 山东威海人, 博士研究生, 主要从事数字图像压缩的研究。E-mail: suiyuping8032@tom.com

and the cost of them, it is essential to reduce the on-board storage capacity and the transmission rate to a minimum^[1-3].

Image compression techniques can be divided into two major families: lossy and lossless. Lossy data compression concedes a certain loss of accuracy in exchange for greatly increased compression ratio. The amount of data reduction achievable with lossless compression is usually limited to about two-to-one by the inherent entropy measurement. To require higher reduction, a lossy compression technique is needed^[4]. The choice of remote sensing image compression algorithm depends on application characteristics: real time or near real time, compression ratio and final image quality requirements. The current popular wavelet-based algorithms such as JPEG-2000 and SPIHT have high performance, but the global complexity of encoders is too high to be applied to the compression of remote sensing images^[5]. According to the above requirements, a new compression scheme with low complexity and good performance is presented, after researching the statistical feature of wavelet coefficients and the entropy of high-frequency sub-bands.

In section 2, the compression algorithm is described. Compression performance results of the algorithm on test images are given in section 3 and section 4 makes a conclusion.

2 Global Compression Scheme

In this paper, it is focused on lossy compression algorithms with three functional modules as depicted in Fig.1: transformation, quantification and encoding.

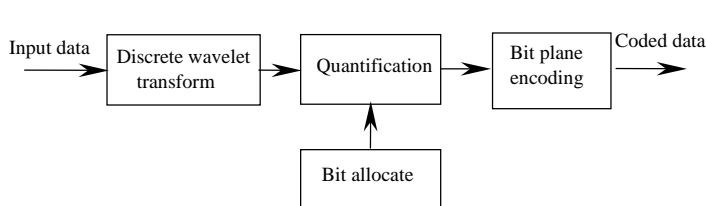


Fig.1 Three modules of the algorithm

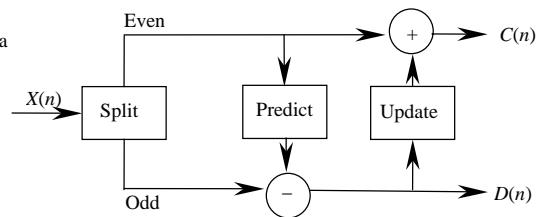


Fig.2 Lifting scheme of wavelet transformation

More details about the algorithm follow.

2.1 Wavelet Transformation

The purpose of the wavelet transformation is to de-correlate for the source. Lifting scheme is adopted. The advantage of the lifting scheme is that it leads to a faster, in-place calculation of the wavelet transform^[6]. A canonical lifting case consists of three stages: split, predict and update, as diagrammed in Fig.2.

1) Split: divides the data set into odd and even elements.

2) Predict: The predict step uses a function that approximates the data set. The difference between the approximation and the actual data replaces the odd elements of the data set.

3) Update: The update step replaces the even elements with an average. In calculating an average the update phase need operate on the differences that are stored in the odd elements.

Experimental results show that biorthogonal wavelets are the best ones for image compression^[7], including float Discrete Wavelet Transform (DWT) and integer DWT. The float DWT gives improved performance at low bit rates, while the integer DWT could presents faster calculation and permits lossless compression^[8]. This module of the algorithm makes use of a three-level, two-dimensional, 5/3 integer DWT.

A two-dimensional DWT is computed by applying the one-dimensional to the rows of image firstly, and then to the columns. Subsequent decomposition stages are applied to the LL sub-band output from the previous stage, producing the pyramidal decomposition^[9]. The flow chart is presented in Fig.3.

After three-level wavelet transformation, ten sub-bands are gained, including one LL3 low frequency and

nine high frequency ones shown in Fig.4. The histogram of nine high-frequency sub-bands is shown in Fig.5. From the histograms it is shown that the distribution of high-frequency sub-bands coefficients complies with generalized Gaussian distribution.

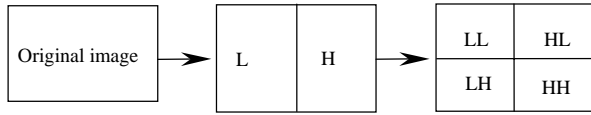


Fig.3 Two-dimensional DWT decomposition

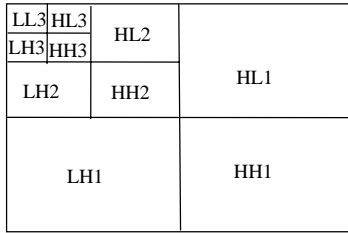


Fig.4 3-Level wavelet decomposition

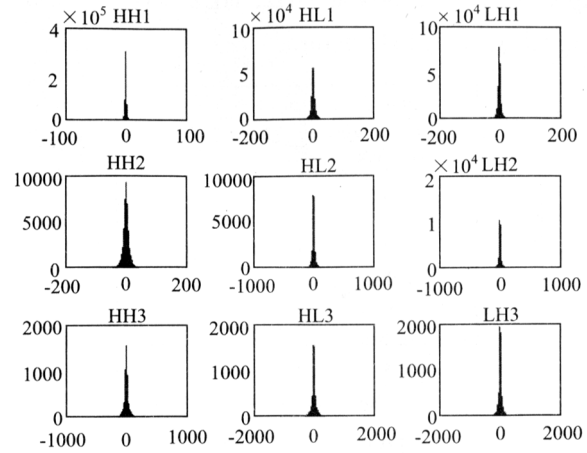


Fig.5 Histogram of nine high-frequency sub-bands

2.2 Quantification

The quantification includes scalar quantification and vector quantification. Due to the complexity constraints, vector quantization is excluded. Only uniform scalar quantization is studied here^[1,10].

2.2.1 Quantification Scheme

LL3 low frequency sub-band is an approximate original image and congregates most energy. The higher energy percentage is the more important sub-band is. So quantification is not implemented with LL3 sub-band. Other nine high frequency sub-bands own tiny energy, furthermore at the same level the energy of horizontal and vertical dimension is more than diagonal, at the different level the bigger the scale is the more energy congregates^[11]. So quantification is processed according to importance degree of the sub-band. Long step is selected for unimportant sub-band and short step for important one. This scheme complies with human visual system. In addition, because many high-frequency coefficients locate near zero, designing an appropriate threshold for each sub-band is more efficient before quantification. Threshold is given in equation (1):

$$Thr = 0.3936 + 0.1829 \cdot (\log n / \log 2) \quad (1)$$

Where Thr is threshold and n is the maximum of the row number and column one.

2.2.2 Bit Allocation

Bit allocation is to choose the best quantification step for sub-band. It is very important to the CR and reconstruction quality.

High frequency sub-bands from wavelet decomposition mainly include the details of image such as veins and verge. HL_i ($i=1,2,3$) contains more high frequency information in the vertical direction; LH_i ($i=1,2,3$) is mainly about horizontal direction information; HH_i ($i=1,2,3$) denotes diagonal high frequency. Fortunately, entropy is a statistical measure of randomness that can be also used to characterize the texture of input image. Entropy is defined in equation(2):

$$H(s) = -\sum_{i=1}^n P(s_i) \cdot \log_2 P(s_i) \quad (2)$$

Where $P(s_i)$ is the probability of the signal s_i .

After testing the energy percentage and entropy value for a set of images' high frequency sub-bands, good near-linear relationship between them at the same decomposition level is demonstrated. Moreover, at different

levels both of them increase with the rising decomposed level. Two examples of the relationship between energy percentage and entropy are showed in Fig.6. The horizontal coordinate is No. of the sub-bands, thereinto sub-band 1,2,3 are from the first decomposed level, denoting HH1, HL1, LH1 in turn; Sub-band 4,5,6 are from the second decomposed level, denoting HH2, HL2, LH2 in turn; Sub-band 7,8,9 are from the third decomposed level, denoting HH3, HL3, LH3 in turn.

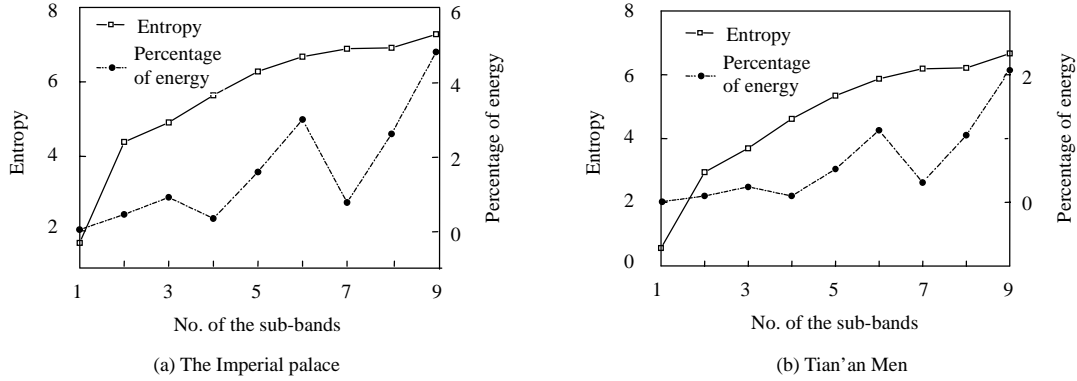


Fig.6 Examples of relationship between energy percentage and entropy

Then the solution of bit allocation is provided:

$$R_i = H(i) \quad (i=1,2,3\dots 9) \quad (3)$$

Where $H(i)$ is entropy value of each high frequency sub-band.

2.3 Encoding

Because low frequency sub-band LL3 is sensitive to the reconstruction quality, lossless compression method-differential pulse code modulation (DPCM) is introduced. Bit plane encoding (BPE) is used for other nine high frequency sub-bands. The encoding sequence is according to the sub-bands' importance degree, i.e. from the third level to the first level, and from LH to HL, HH at the same level.

$BitDepth$ in equation (4) denotes the maximum number of bits needed to specify the magnitude of any coefficient in the sub-band:

$$BitDepth = \lceil \log_2(1 + \max |x|) \rceil \quad (4)$$

Bit plane b is the b^{th} bit of the two's-complement integer representation of each coefficient. Here, bit plane index $b=0$ corresponds to the least significant bit. The BPE proceeds from most-significant bit to least significant bit in the same sub-band, thus b decreases from one bit plane to the next, beginning with $b=BitDepth$ and ending with $b=BitDepth-H(i)$.

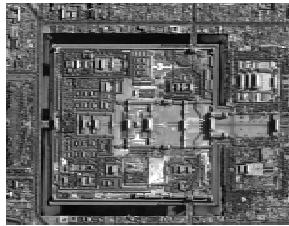
According to the analysis of wavelet coefficients, it is known that the coefficient number bigger than $2^{BitDepth}$ is a few. In order to increase Compression Ratio (CR), the coordinates of non-zero coefficients were registered in the bit plane $b=BitDepth$, and run-length encoding and Huffman encoding were proceeded for other bit planes.

3 Experimental Results

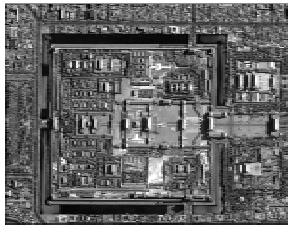
All simulations experiments are based on software and experimental environment follows: 64 processor, 512MB EMS memory, windows XP, Matlab 7.0. In order to compare my algorithm with the current JPEG technique, a set of 8-bit, frame-mode image are used. Tested images are listed in Tab.1. Two examples of tested images and reconstructed images are given in Fig.7 and Fig.8. Tab.2 shows quantitative comparison of my approach and JPEG.

From Fig.7, Fig.8 and Tab.2, it can be seen that there is little distortion between the reconstructed and original image for all tested images and all Peak Signal To Noise Ratio (PSNR) are higher than 34dB. CR depends on

images' complicated degree. The more complexity the texture is, the lower the CR is. Experimental results demonstrate that both PSNR and CR are all a little better than JPEG.

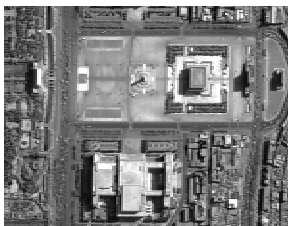


(a) Original image

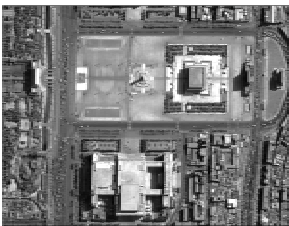


(b) Reconstructed image

Fig.7 Imperial palace



(a) Original image



(b) Reconstructed image

Fig.8 Tian'an Men

Table 1 List of tested images

Image	Source	Size	bpp
Wahsat	SPOT	512×512	8
Tian'an men	QuickBird	1749×1348	8
The imperial palace	QuickBird	1249×1024	8
F1	MSS	300×186	8
Pyrimid	IKONOS	674×576	8
Tokyo	IKONOS	615×800	8

Table 2 Quantitative comparison of my approach and JPEG

Test Images	My approach		JPEG	
	CR	PSNR	CR	PSNR
Wahsat	10.06	37.40	7.58	37.41
Tian'an men	6.85	36.92	5.39	36.56
The imperial palace	3.35	34.26	3.29	33.51
F1	3.87	34.44	3.85	33.77
Pyramid	6.93	35.75	5.08	35.21
Tokyo	5.97	35.50	4.71	35.53

4 Conclusions

The information in remote sensing images is usually valuable, so too high compression ratio is inadvisable. In this paper, the changing trend of entropy and energy percentage of each sub-band is studied and good near-linear relationship between them is found at the same level. The statistical characteristic of wavelet coefficients is made fully use of in the dynamic bit allocation and bit plane encoding. Tests show that this algorithm can present graceful reconstructed images for both complicated texture images and relative planar ones. A C software implement is expected to be available soon, and DSP hardware implementation is currently under development.

References:

- [1] Catherine LAMBERT-NEBOUT , Gilles MOURY. A survey of on-board image compression for CNES space missions [J]. **IGARSS's 99 Proceedings** , 1999 , 4 : 2032-2034.
- [2] WU Wen-bo ,YANG ZHI-gao ,MA Guo-rui *et al*. Remote sensing image compression based on a morphological wavelet coding [J]. **Journal of Image and Graphics** , 2005 , 10(7) : 867-872. (in Chinese)
- [3] TIAN Bao-feng , XU Shu-yan , SUN Rong-chun , *et al*. A lossy compression algorithm of remote sensing image suited to space-borne application [J]. **Optics and Precision Engineering** , 2006 , 14(4) : 725-730. (in Chinese)
- [4] YEH Pen-Shu , VENBRUX Jack , BHATIA Prakash , *et al*. A real-time high performance data compression technique for space applications [J]. **IGARSS's 2000 Proceedings** , 2000 , 2 : 612-614.
- [5] ARISOTChristophe P ,ANTONINI Marc ,BARLAUD. Michel EBWIC :a low complexity and efficient rate constrained wavelet image coder [J]. **Image Processing, 2000 Proceedings** , 2000 , 1 : 653-656.
- [6] SWELDENS W. The lifting scheme : a construction of second generation wavelets [J]. **SIAM Journal of Mathematical Analysis** , 1997 , 29(2) : 511-546.
- [7] XU Xin-feng ,DONG Gui-hua ,FENG Yi *et al*. A new spaceborne compression approach for remote sensing imagery[J]. **ICO20: Remote Sensing and Infrared Devices and Systems** , 2006 , 6031 : 6031X-1-6031X-8.

24 : 185-188.

- [4] SU Xian-yu , ZHOU Wen-sen , VON BALLY C , *et al.* Automated phase-measuring profilometry using defocused projection of a Ronchi grating [J]. **Optics Communications** , 1992 , **94**(6) : 561-573.
- [5] Halious Maurice , Liu Hsin-Chu. Optical three-dimensional sensing by phase measurement profilometry [J]. **Optics and Lasers in Engineering** , 1989 , **11**(3) : 185-215.
- [6] 苏显渝, 周文胜. 采用罗奇光栅离焦投影的位相测量剖面术[J]. 光电工程, 1993, **20**(4) : 8-11.
SU Xian-yu , ZHOU Wen-sheng. Phase-Measuring Profilometry Using Defocused Projection of the Ronchi Grating [J]. **Opto-Electronic Engineering** , 1993 , **20**(4) : 8-11
- [7] 宋万忠, 苏显渝, 游志胜. 相位测量轮廓术中的距离像配准[J]. 光电工程, 2004, **31**(4) : 42-45.
SONG Wan-zhong , SU Xian-yu , YOU Zhi-sheng. Registration algorithm of range images in phase-measuring profilometry [J]. **Opto-Electronic Engineering** , 2004 , **31**(4) : 42-45.
- [8] Guan C , Hassebrook L , Lau D. Composite structured light pattern for three-dimensional video [J]. **Optics Express** , 2003 , **11**(5) : 406-417.
- [9] 岳慧敏, 苏显渝. 复合相位测量轮廓术研究[J]. 激光杂志, 2006, **27**(1) : 22-23.
YUE Hui-min , SU Xian-yu. Study on composite phase measuring profilometry [J]. **Laser Journal** , 2006 , **27**(1) : 22-23.
- [10] Xue Lian , Su Xianyu. Phase-unwrapping algorithm based on frequency analysis for measurement of a complex object by the phase-measuring-profilometry method [J]. **Opt. Eng** , 2001 , **40**(4) : 637-643.
- [11] Su Xianyu , Chen Wenjing. Reliability-guided phase unwrapping algorithm: a review [J]. **Optics and Lasers in Engineering** , 2004 , **42**(3) : 245-261.
- [12] 苏显渝, 陈文静, 曹益平, 等. 参数图导向的相位展开方法[J]. 光电子·激光, 2004, **15**(4) : 463-467.
SU Xian-yu , CHEN Wen-jing , CAO Yi-ping , *et al.* Phase Unwrapping Algorithm Based on the Oriented Parameter Map [J]. **Journal of Optoelectronics·laser** , 2004 , **15**(4) : 463-467.
- [13] ZHOU Wen-sen , SU Xian-yu. A direct mapping algorithm for phase-measuring profilometry [J]. **J.Mod.Opt** , 1994 , **41**(1) : 89-94.

~~~~~

( 上接 65 页 )

- [8] YEH Pen-Shu , ARMBRUSTER Philippe , KIELY Aaron , *et al.* The new CCSDS image compression recommendation [C]// **Aerospace, 2005 IEEE Conference**. [S.l.] : IEEE , 2005 : 4138-4145.
- [9] MALLAT S G. A theory for multiresolution signal decomposition : the wavelet representation[J]. **IEEE Transactions on Pattern Analysis and Machine Intelligence** , 1989 , **11**(7) : 674-693.
- [10] PARISOT C , ANTONINI M , BARLAUD M , *et al.* On board strip-based wavelet image coding for future space remote sensing missions [J]. **IGARSS's 2000 Proceedings** , 2000 , **6** : 2651-2653.
- [11] KONG Ya-ping , ZHANG Xiao-lin , LIU Rong-ke. Improvement on strip-based wavelet compression coding for remote sensing image [J]. **Telemetry & Telecontrol** , 2003 , **24**(6) : 39-42. (in Chinese)